Electronic Supplementary Material (ESI) for Physical Chemistry Chemical Physics.
This journal is © the Owner Societies 2023

Nanoscale Characterization of Heterogeneous Interfacial Oxidation layer of Graphene/Cu based on SEM Electron Beam Induced Reduction Effect

Panpan Feng [a, b], *Dan Zhang* [a, b, *], *Peng Zhang* [c], *You Wang* [d, e], *Yang Gan* [a, b, *]

[a] School of Chemistry and Chemical Engineering, Harbin Institute of Technology, Harbin 150001, People's Republic of China

[b] MIIT Key Laboratory of Critical Materials Technology for New Energy Conversion and Storage, School of Chemistry and Chemical Engineering, Harbin Institute of Technology, Harbin 150001, People's Republic of China

[c] Manufacturing Engineering for Aviation and Aerospace, School of Mechatronics Engineering, Harbin Institute of Technology, Harbin 150001, People's Republic of China

[d] Key Laboratory of Micro-Systems and Micro-Structures Manufacturing, Ministry of Education, Harbin Institute of Technology, Harbin 150001, People's Republic of China

[e] Materials Physics and Chemistry Department, Harbin Institute of Technology, Harbin 150001, People's Republic of China

[*] E-mail: ygan@hit.edu.cn, zhangd@hit.edu.cn

Contents

Table S1-3 XPS peak area and FWHM of Cu2p3/2, CuLMM, and O1s peaks of graphene covered area within EBI region of the Gr/Cu sample (shown in Figure 1) treated under different conditions.

Table S4: XPS atomic percent of C, O, Cu for the Gr/Cu sample (shown in Figure 1) treated under different conditions.

Table S5 Irradiation time, electron dose and V*acc* (the energy of the incident electrons) required for the reduction of interfacial oxide layer.

Fig. S1 SEM image and Raman spectra of different graphene covered area within EBI regions of Gr/Cu samples subjected to EBI for different time.

Fig. S2 C1s spectra of the same region as shown in **Figure 2** for a Gr/Cu sample and HRTEM image.

Fig. S3 HRTEM image and XPS spectra of Gr/Cu samples annealed in H_2/Ar.

Fig. S4 SEM images of Gr/Cu samples (treated under different thermal oxidation conditions) before and after EBI for 30 min.

Fig. S5 SEM images of Gr/Cu samples (stored under low humidity at room temperature for different time) before and after EBI for 30 min.

Fig. S6 SEM image and AFM topography showing the EBI induced carbon deposited region on a Cu foil as well as the AFM line profile.

Fig. S7 The plot of CV and thickness of carbon deposition layer as a function of EBI time for the same EBI region of graphene covered area of Gr/Cu sample shown in figure 1.

Fig. S8 XPS spectra obtained at the EBI region of Gr/Cu sample after 12 h EBI.

Fig. S9 XPS spectra of EBI region on Cu foil before and after EBI.

Fig. S10 Cross-sectional HRTEM image and TEM-EDS elemental maps of Cu and O.

Fig. S11 The statistical values of the thickness (from cross-sectional HRTEM characterization) of interfacial oxide layer of graphene covered region and surface oxide layer of Cu substrate of Gr/Cu samples.

Fig. S12 Low magnification cross-sectional TEM images of graphene covered regions and Cu surface region of Gr/Cu samples after different treatments.

Fig. S13 SEM images of the same region of a fully covered Gr/Cu sample before EBI and subjected to EBI for different time.

Fig. S14 EBSD inverse pole figure (IPF) coloring orientation map, IPF triangle and SEM image of a region for polycrystalline Gr/Cu sample stored under low humidity for 14 days, and SEM images of selected areas of three grains within the region before and after EBI.

Fig. S15 SEM and HRTEM images of Gr/Cu samples (stored under low humidity for different time and subjected to different thermal oxidation) after 30 min EBI.

Fig. S16 The electron dose per area vs irradiation time curves for the EBI region of A1, A2, A3 and A4 at different Vacc.

Fig. S17 SEM images of a Gr/Cu sample before and after EBI as well as Raman mapping images of the same region after EBI.

Table S1 XPS peak area and FWHM of Cu2p3/2 peaks of graphene covered area within EBI region of the Gr/Cu sample (shown in Figure 1) treated under different conditions

Experimental conditions	Binding energy (eV)	FWHM (eV)	Peak area	Peak area ratio between Cu and Cu_2O+CuO
Before EBI: oxidation at 50 °C for 60 min	Cu:932.4	0.9	5229.7	1.3
	Cu_2O: 932.6	1.9	2521.8	
	CuO: 934.4	3.2	1386.2	
EBI for 30 min	Cu: 932.4	1.1	4592.8	2.4
	Cu_2O: 932.8	2.0	1908.9	
After EBI: oxidation at 50 °C for 30 min	Cu: 932.4	1.1	4241.7	1.9
	Cu_2O: 932.8	3.4	2200.0	

Table S2 XPS peak area and FWHM of CuLMM peaks of graphene covered area within EBI region of the Gr/Cu sample (shown in Figure 1) treated under different conditions

Experiments conditions	Binding energy (eV)	FWHM (eV)	Peak area	Peak area ratio between Cu and Cu_2O
Before EBI: oxidation at 50 °C for 60 min	Cu_2O: 570.6	4.6	73920.3	--
	CuO: 569.3	4.0	61232.3	
EBI for 30 min	Cu_2O: 570.6	6.6	522843.1	1.1
	Cu: 568.3	2.7	580783.4	
After EBI: oxidation at 50 °C for 30 min	Cu_2O: 570.6	6.0	298659.3	0.9
	Cu: 568.3	2.3	270326.1	

Table S3 XPS peak area and FWHM of O1s peaks of graphene covered area within EBI region of the Gr/Cu sample (shown in Figure 1) treated under different conditions

Experimental conditions	Binding energy (eV)	FWHM (eV)	Peak area	Peak area percent of Cu_2O or CuO
Before EBI: oxidation at 50 °C for 60 min	CuO:530.7	1.7	6816.0	0.15 (CuO)
	C-O-H:531.7	1.5	31953.3	
	C-O-C:532.8	1.8	6010.6	
EBI for 30 min	Cu_2O:530.2	1.7	7537.9	0.15 (Cu_2O)
	C-O-H:531.7	1.6	29267.3	
	C-O-C:532.8	1.7	14239.6	
After EBI: oxidation at 50 °C for 30 min	Cu_2O:530.2	2.2	10055.3	0.20 (Cu_2O)
	C-O-H:531.7	1.9	37184.4	
	C-O-C:532.8	2.6	3313.8	

Table S4: XPS atomic percent of C, O, Cu for the Gr/Cu sample (shown in Figure 1) treated under different conditions

Experimental conditions	**C** (Atomic %)	**O** (Atomic %)	**Cu** (Atomic %)
Before EBI: oxidation at 50 °C for 60 min	73.3	21.8	4.9
EBI for 30 min	38.3	8.1	53.6
After EBI: oxidation at 50 °C for 30 min	44.0	18.0	38.0

Table S5 Irradiation time, electron dose and V*acc* (the energy of the incident electrons) required for the reduction of interfacial oxide layer (or the contrast reversal) in the EBI regions with different size.

Irradiation area	1 kV		3 kV		5 kV		8-10 kV	
	τ (min)	*dose* ($e^-/\mu m^2$)	τ (min)	*dose* ($e^-/\mu m^2$)	τ (min)	*dose* ($e^-/\mu m^2$)	τ (min)	*dose* ($e^-/\mu m^2$)
A_1:150×112.5 μm^2	115	5×10^{10}	120	6×10^{10}	120	6×10^{10}	130	6×10^{10}
A_2:50×37.5 μm^2	25	3.3×10^{11}	25	3.3×10^{11}	30	4×10^{11}	45	6×10^{11}
A_3:20×15 μm^2	8	2×10^{11}	10	2.5×10^{11}	10	2.5×10^{11}	15	3.7×10^{11}
A_4:5×3.75 μm^2	1	1.2×10^{12}	1	1.2×10^{12}	1	1.2×10^{12}	7	8.4×10^{12}
A_5:2.5×0.2 μm^2					0.17 (10 s)	$<3\times10^{12}$		

Note about the selection of SE detector and the effect of V*acc* on irradiation damage to graphene (Fig. S1)

Although the ET detector—the standardly equipped detector for SEs imaging besides the In-lens detector—can also be applicable for observation of contrast reversal, we still recommend In-lens detector instead of ET detector because of two reasons. Firstly, imaging with the ET detector for observation of contrast reversal is reliable only at large working distance (WD) (>30 mm) and high acceleration voltage (V*acc*) (≥15 kV) because of strong interference of electron channel effect on the contrast of ET images for polycrystalline Cu;[3] conversely, the In-lens detector is less susceptible to this problem. Secondly, ET imaging at high V*acc* may increase the risk of irradiation damage to graphene. In this study, images were recorded at low V*acc* up to 5 kV with the In-lens detector so that no electron beam induced irradiation damage occurred as confirmed by Raman characterization of graphene subjected to 50 min EBI (Fig. S1b). In addition, the G and 2D peaks did not widen after 30min EBI, indicating that graphene was not oxidized to graphene oxide.[4] Furthermore, we found that imaging at 5 kV affords balance of good image contrast of graphene and proper WD for safe SEM operation. In addition, for graphene covered area of Gr/Cu samples before EBI (Fig. S1c), the value of $I_{2D}/_{G}$ is larger than or equal to 2, indicating that single layer graphene was grown on Cu substrate.

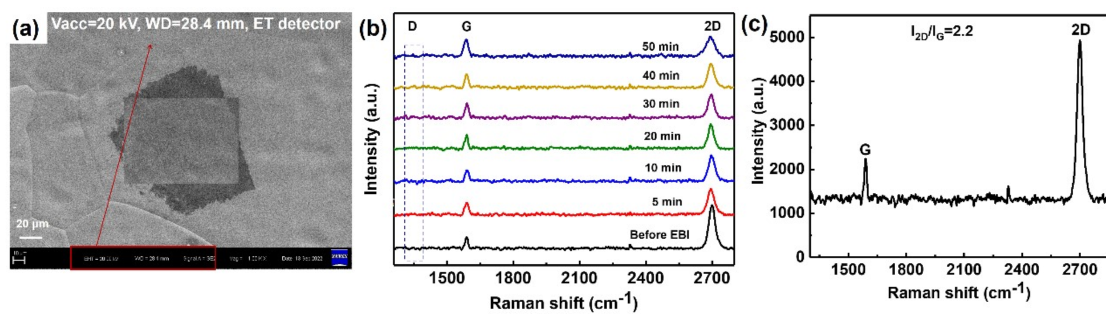

Figure S1 (a) SEM image of Gr/Cu captured with ET detector after EBI for 30 min. (b) Raman spectra of different graphene covered area within EBI regions of Gr/Cu samples subjected to EBI for different time. (c) Raman spectra of graphene covered area as shown in Figure 1.

Note about whether graphene is apart from Cu substrate after EBI (Fig. S2)

After EBI, the interfacial oxide layer became thinner and discontinuous, and the binding energy of graphene increased to 284.7 eV as shown in Fig. S2, which is close to the binding energy of graphene coupled with substrate.[1] The binding energy of graphene for the sample before EBI and after EBI (subjected to further thermal oxidation) decreased. It has been reported that the interaction between graphene and the underlying Cu could be decoupled by the intercalation of a thin interfacial oxide layer, and it can also be recoupled when the intercalated oxygen or the interfacial oxide layer disappeared. [1, 2] Therefore, after EBI, the interaction between graphene and the underlying Cu was enhanced due to the reduction of interfacial oxide layer induced by EBI, so that graphene will not be apart from Cu substrate. The HRTEM image of the interface for Gr/Cu sample after EBI also demonstrated that graphene was not apart from the Cu substrate. During EBI, the diffusion of generated oxygen will not be affected.

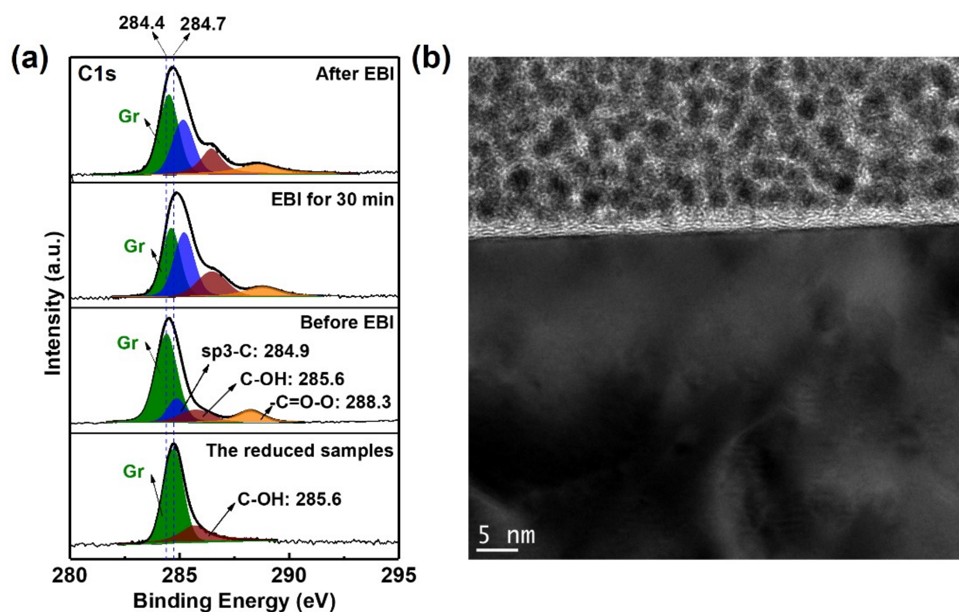

Figure S2 (a) C1s spectra of the same region as shown in **Figure 2** for a Gr/Cu sample before EBI, EBI for 30 min and after further thermal oxidation and (b) HRTEM image of the interface of Gr/Cu sample after EBI for 30 min. Before EBI: sample annealed in H_2/Ar and thermally oxidized in air at 50 °C for 60 min. EBI: 30 min, V*acc*=5 kV, irradiation dose =4×10^{11} e^- /μm^2. After EBI: sample thermally oxidized in air at 50 °C for 30 min.

Note about the characterization of the interface of Gr/Cu samples annealed in H_2/Ar (Fig. S3)

As shown Fig. S3a, the interfacial oxide layer cannot be observed at the interface of Gr/Cu samples annealed in H_2/Ar in HRTEM image. XPS spectra of as-grown Gr/Cu samples was also measured. The binding energy of graphene (284.7 eV) has not changed. Only the peak of Cu was detected on XPS spectra of Cu2p3/2. For O1s spectra, a weak peak of Cu_2O was observed because of the air exposure for the Gr/Cu sample during sample preparation. The peak area percentage of Cu_2O for as-grown Gr/Cu samples was also less than that for oxidized samples before EBI. Therefore, the Cu substrate underlying graphene is not oxidized.

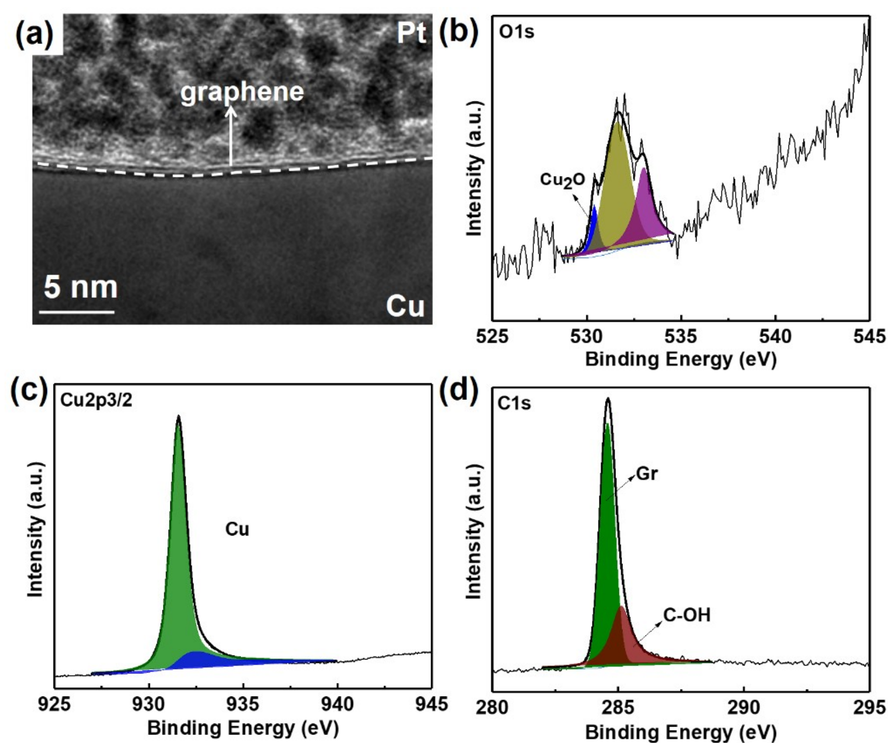

Figure S3 HRTEM image and XPS spectra of Gr/Cu samples annealed in H_2/Ar.

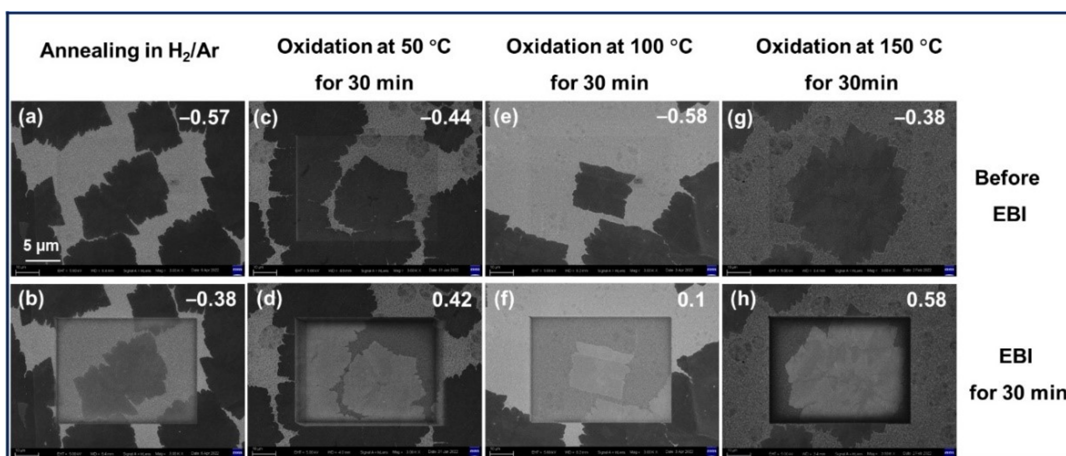

Figure S4 SEM images of Gr/Cu samples (treated under different thermal oxidation conditions) before and after EBI for 30 min. (a-b) Annealing in H_2/Ar. (c-d) Oxidation at 50 °C for 30 min. (e-f) Oxidation at 100 °C for 30 min. (g-h) Oxidation at 150 °C for 30 min. The values given in the images are CV.

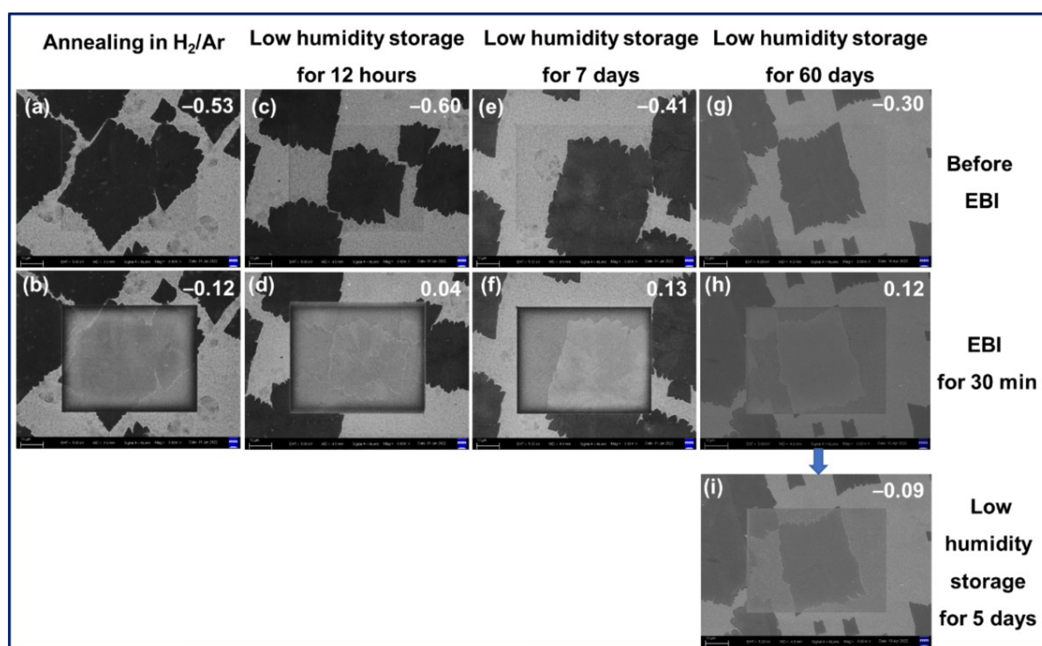

Figure S5 SEM images of Gr/Cu samples (stored under low humidity at room temperature for different time) before and after EBI for 30 min. (a-b) Annealing in H_2/Ar. (c-d) Stored for 12 h. (e-f) Stored for 7 days. (g-h) Stored for 60 days. (i) Low humidity storage for 5 days after 30 min EBI.

Note about the effect of carbon deposition on SEM image contrast (Fig. S6-8)

The following results and analysis show that carbon deposition during EBI process and imaging cannot cause the observed contrast reversal. Provided that the contrast reversal is caused by the carbon deposition, it should be observed for any graphene covered regions after EBI. However, we did not observe contrast reversal after EBI for both Gr/Cu samples without interfacial oxide layer that was annealed in H_2/Ar (Fig. S4-5) and Gr/Cu samples with thicker interfacial oxide layer (Fig. S15). Nonetheless, we note that carbon deposition decreases the overall contrast of the whole EBI region; this was considered for selecting the proper EBI time for various samples including those shown in Fig. 2. More results showing the influence on CV and the thickness of the carbon deposition layer are given in Fig. S6-8. The thickness of carbon deposition was determined by AFM characterization as illustrated in Fig. S6. With the increase of EBI time, CV values gradually increased and reached the maximum value at 30 min (Fig. S7). However, the carbon deposition layer can decrease the SEM image contrast, and the thickness of which is positively correlated with EBI time. Therefore, the CV gradually flattened out as the EBI time continued to increase. when the carbon layer completely masks the contrast of graphene, the CV is close to 0. As illustrated in Fig.S5, the EBI time is 90 min as CV≈0. Finally, and interfacial oxides cannot be detected by the XPS equipment (Fig. S8).

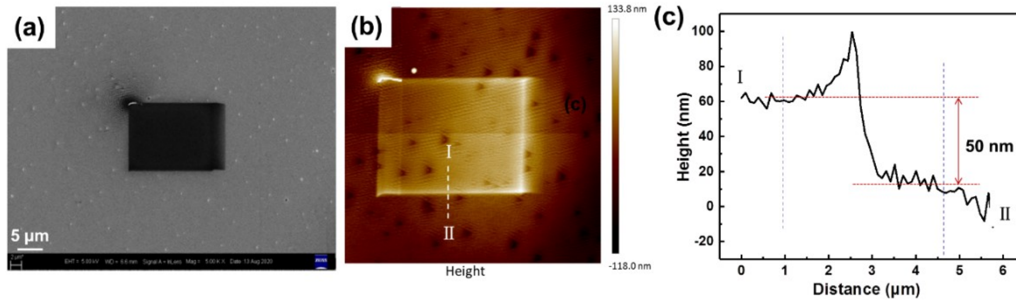

Figure S6 SEM image and AFM topography showing the EBI induced carbon deposited region on a Cu foil as well as the AFM line profile. (a) SEM image. (b) AFM topography. (c) The line profile along I-II in b. EBI time: 12 h, V*acc*: 5 kV**.**

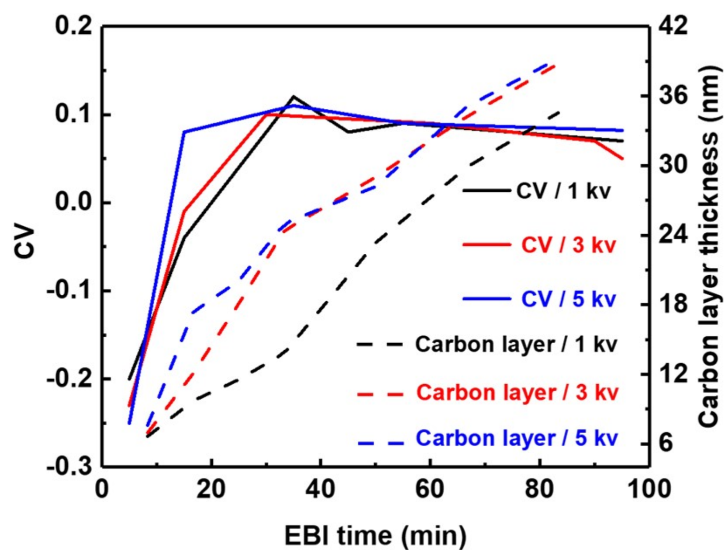

Figure S7 The plot of CV and thickness of carbon deposition layer as a function of EBI time for the same EBI region of graphene covered area of Gr/Cu sample shown in figure 1. WD: 6 mm

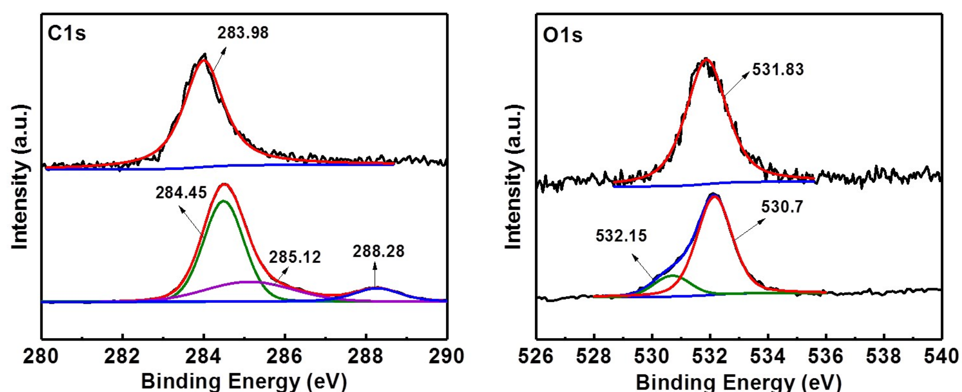

Figure S8 XPS spectra obtained at the EBI region of Gr/Cu sample after 12 h EBI.

Note about the effect of carbon deposition on SEM image contrast (Fig. S9)

The oxide layer on the surface of Cu substrate can also be reduced by EBI. We have measured XPS spectra of Cu2p3/2, O1s and C1s for Cu foil without graphene, and evaluated the change of CuO before and after EBI. There are two Cu2p3/2 peaks of 932.4 eV (Cu), 934.4 eV (CuO) before EBI, the peak of 934.4 eV (CuO) disappears after EBI. The O1s peak shifts from 530.7 eV (CuO) to 530.2 eV (Cu_2O) after EBI. The peak of 285.6 eV (C-OH) appeared and the intensity of the peak of 288.3 eV (-C=O-O) increased after EBI because a carbon layer was deposited on the surface within EBI region. Therefore, the Cu oxides (CuO) was reduced after EBI. SEM image of Cu substrate after EBI can be found in Figure 2b in previous manuscript. Because the oxide layer is still thick and continuous compared with interfacial oxide layer after the same time of EBI, the brightness of Cu substrate within EBI region has not increased.

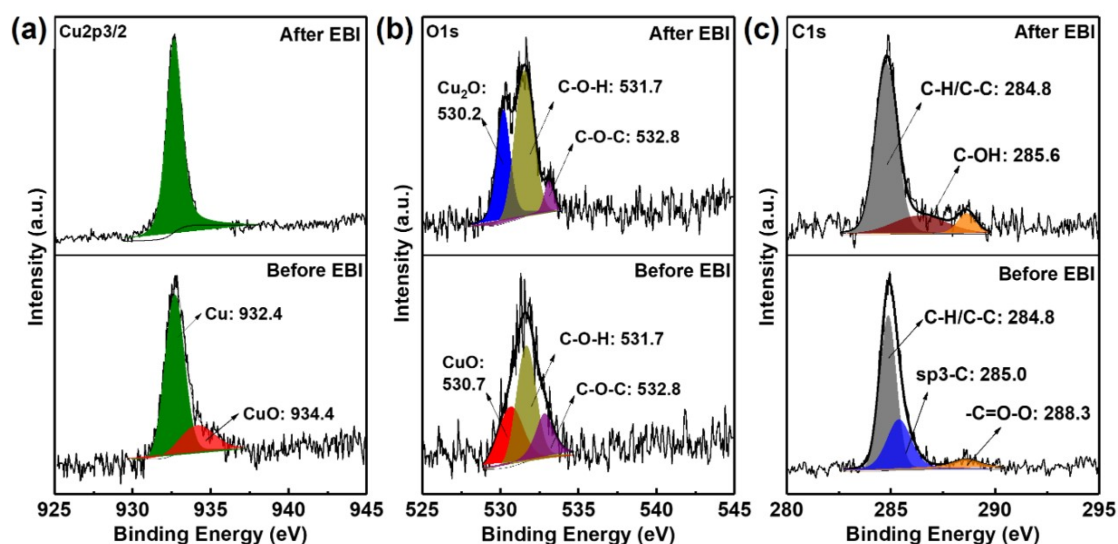

Fig. S9 XPS spectra of EBI region on Cu foil before and after EBI.

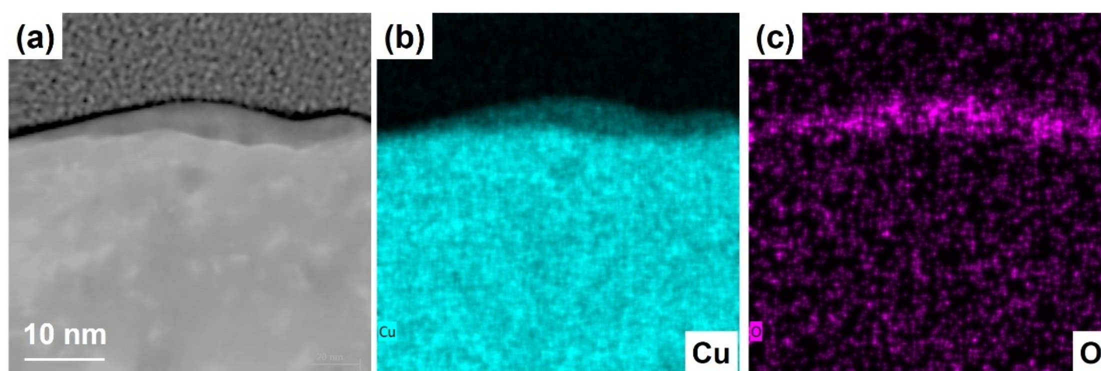

Figure S10 Cross-sectional HRTEM image (a) and TEM-EDS elemental maps of Cu (b), O (c) of interfacial oxidation layer in the cross-sectional view.

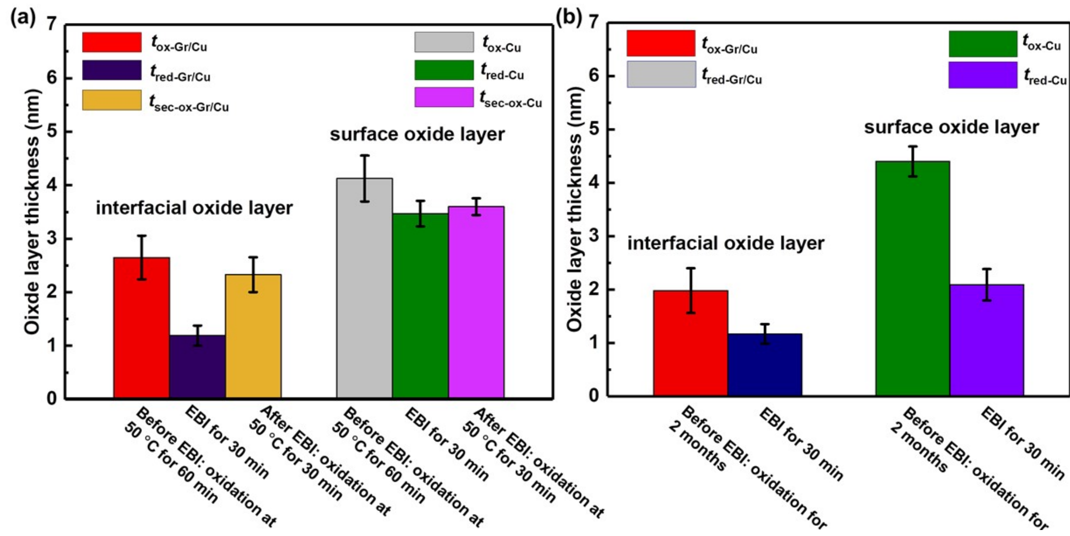

Figure S11 The statistical values of the thickness (from cross-sectional HRTEM characterization) of interfacial oxide layer of graphene covered region and surface oxide layer of Cu substrate of Gr/Cu samples. (a) Thermally oxidized Gr/Cu sample. (b) Low humidity stored Gr/Cu sample at room temperature. $t_{\text{ox-Gr/Cu}}$: thickness of interfacial oxide layer of Gr/Cu sample before EBI. $t_{\text{ox-Cu}}$: thickness of surface oxide layer of Gr/Cu sample before EBI. $t_{\text{red-Gr/Cu}}$: thickness of interfacial oxide layer of Gr/Cu sample after EBI. $t_{\text{red-Cu}}$: thickness of surface oxide layer of Gr/Cu sample after EBI. $t_{\text{sec-ox-Gr/Cu}}$: thickness of interfacial oxide layer after following thermal oxidation; $t_{\text{sec-ox-Cu}}$: thickness of surface oxide layer of Gr/Cu sample after following thermal oxidation.

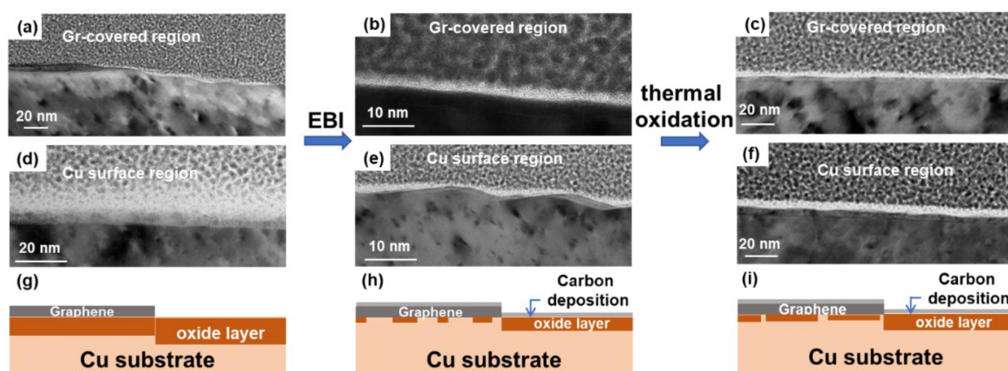

Figure S12 Low magnification cross-sectional TEM images of graphene covered regions and Cu surface region of Gr/Cu samples after different treatments. (a, d) Before EBI: the sample subjected to annealing in H_2/Ar and thermal oxidation at 50 °C for 60 min. (b, e) EBI: 30 min, V*acc*=5 kV, irradiation dose =4×10^{11} e^- /μm^2. (c, f) After EBI: the sample subjected to oxidation at 50 °C for 30 min. (g-i) Illustration of Gr/Cu samples showing graphene covered regions and Cu surface regions with interfacial and surface oxides.

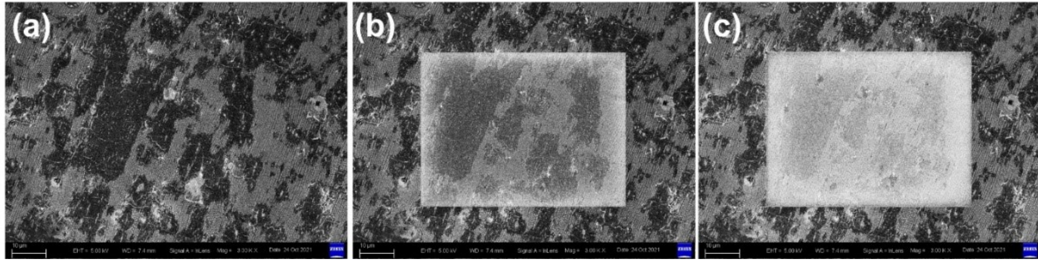

Figure S13 SEM images of the same region of a fully covered Gr/Cu sample before EBI and subjected to EBI for different time. (a) Before EBI. (b) EBI for 15 min. (c) EBI for 30 min.

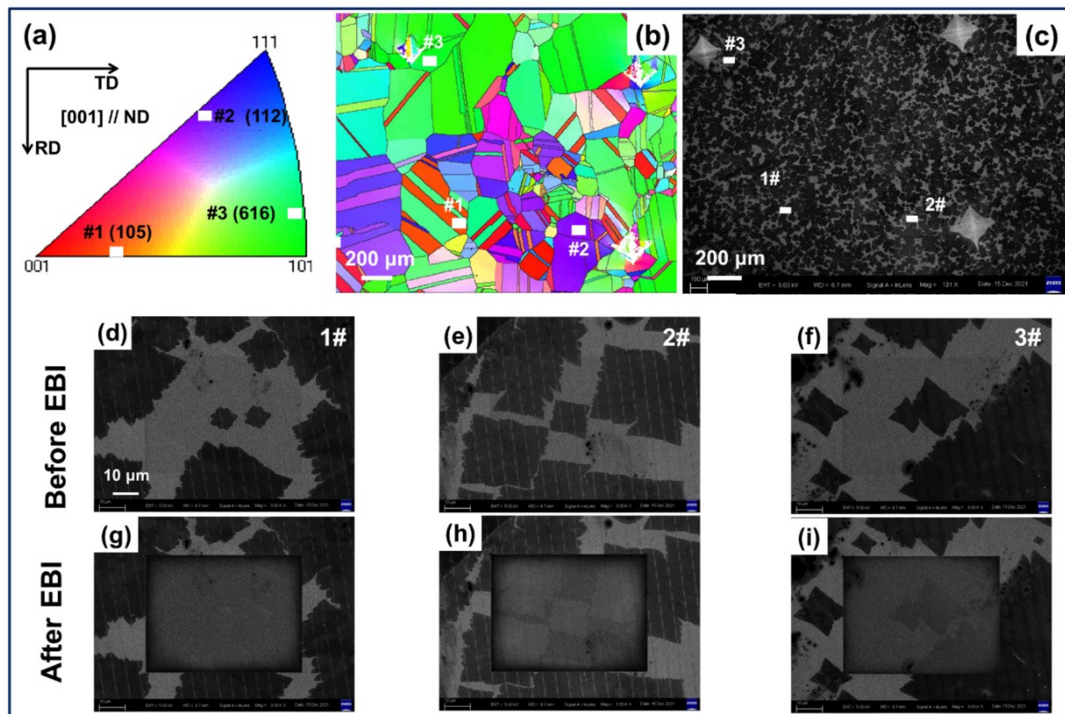

Figure S14 EBSD inverse pole figure (IPF) coloring orientation map, IPF triangle and SEM image of a region for polycrystalline Gr/Cu sample stored under low humidity for 14 days, and SEM images of selected areas of three grains within the region before and after EBI. (a) IPF triangle. (b) IPF coloring orientation map. (c) SEM image of the region. (d, g) Grain #1. (e, h) Grain #2. (f, i) Grain #3.

Low humidity stored Gr/Cu sample

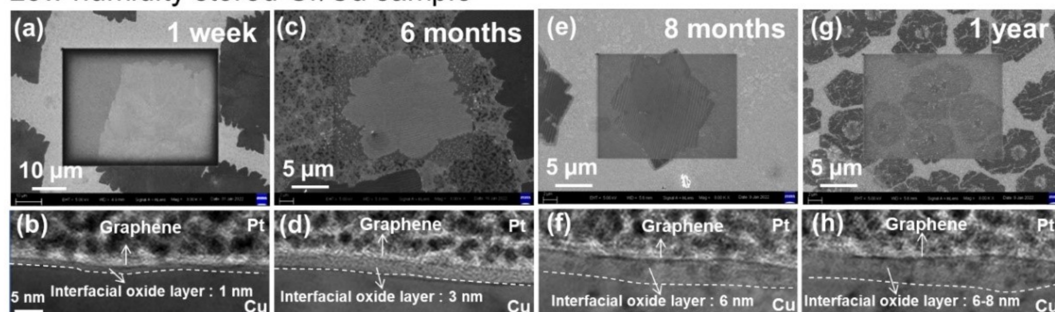

Thermally oxidized Gr/Cu sample

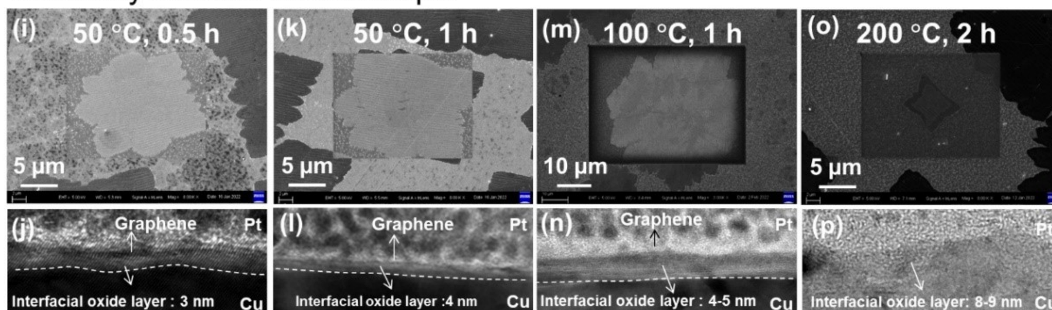

Figure S15 SEM and HRTEM images of Gr/Cu samples (stored under low humidity for different time and subjected to different thermal oxidation) after 30 min EBI. (a, b) Low humidity storage for 1 week. (c, d) Low humidity storage for 6 months. (e, f) Low humidity storage for 8 months. g, h) Low humidity storage for 1 year at room temperature. Thermal oxidation conditions: (i, j) 50 °C, 0.5 h. (k, l) 50 °C, 1 h. (m, n) 100 °C, 1 h. (o, p) 200 °C, 2 h.

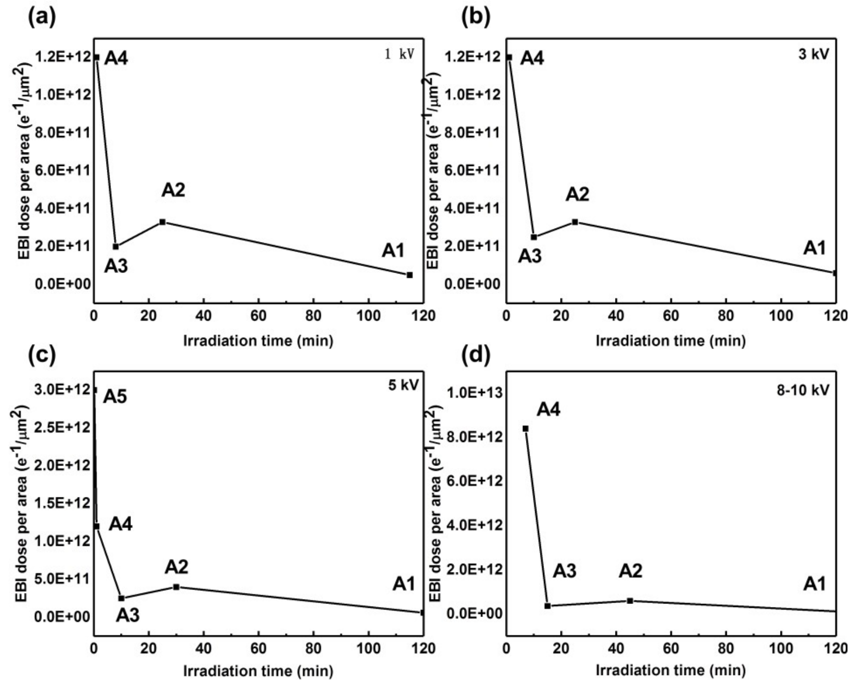

Figure S16 The electron dose per area vs irradiation time curves for the EBI region of A1, A2, A3 and A4 at different Vacc. (a) 1 kV; (b) 3 kV; (c) 5 kV; (d) 8-10 kV.

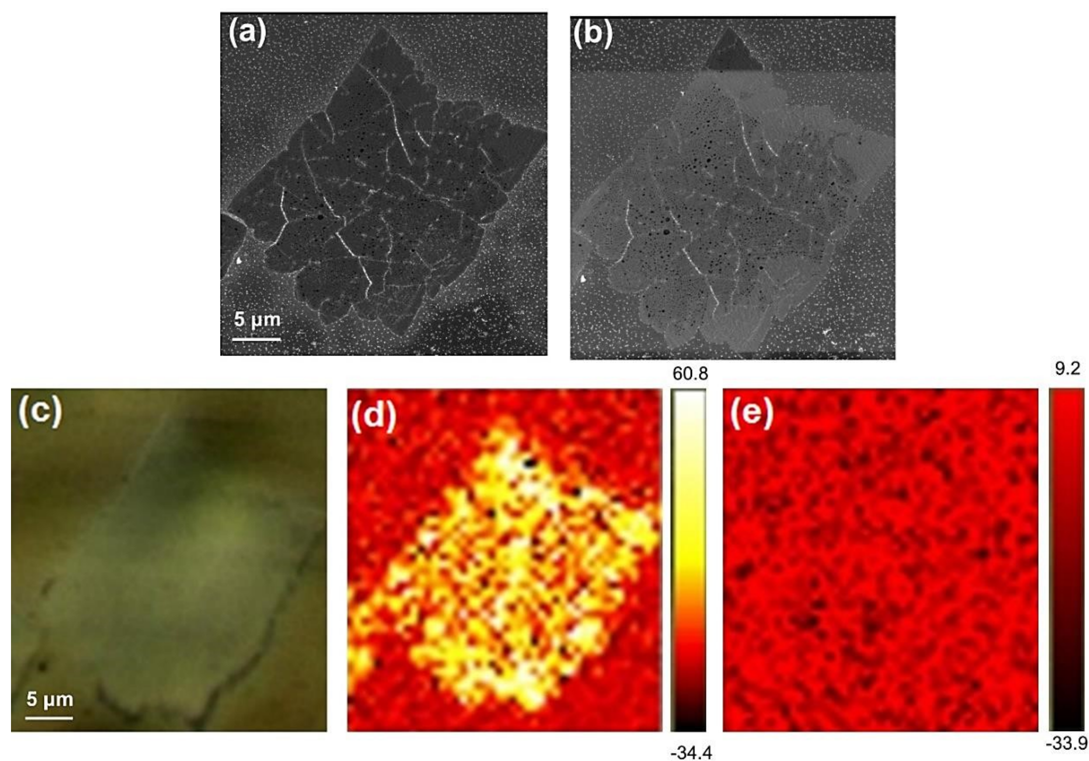

Figure S17 SEM images of a Gr/Cu sample before and after EBI as well as Raman mapping images of the same region after EBI. (a) SEM image before EBI. (b) SEM image after EBI. (c) Raman optical image. (d) Raman mapping image at 2700 cm^{-1} (2D peak of graphene). (e) Raman mapping image at 903 cm^{-1} (Cu_2O).

References

1. Kidambi P. R., Bayer B. C., Blume R., Wang Z.-J., Baehtz C., Weatherup R. S., Willinger M.-G., Schloegl R., Hofmann S., *Nano lett.*, 2013, **13**, 4769-4778.
2. Lu, Ang Y., Wei, Sung B., Wu, Chih Y., Hernandez, Yenny, Chen, Tzu Y., Liu, Te H., Pao, Chun W.i, Chen, Fu R., Li, Lain J., Juang, Zhen Y., *RSC Advances*, 2012, **2**(7), 2046-2069.
3. L. Huang, D. Zhang, F.-H. Zhang, Y.-D. Huang and Y. Gan, *Materials Research Express*, 2019, **6**, 085604.
4. B. O. Konstantin N. K, Hannes C. S., and I. A. A. Robert K. P., and Roberto C., *Nano lett.*, 2008, **8**, 36-41.